HHS Public Access

Author manuscript

Mol Psychiatry. Author manuscript; available in PMC 2024 April 25.

Published in final edited form as:

Mol Psychiatry. 2023 December ; 28(12): 5228–5236. doi:10.1038/s41380-023-02158-0.

Sex matters: Acute functional connectivity changes as markers of remission in late-life depression differ by sex

James D. Wilson, PhD[*,1], **Andrew R. Gerlach, PhD**[*,2], **Helmet T. Karim, PhD**[2,3], **Howard J. Aizenstein, MD, PhD**[2,3], **Carmen Andreescu, MD**[2]

[1]Department of Mathematics and Statistics, University of San Francisco, San Francisco, CA, USA

[2]Department of Psychiatry, University of Pittsburgh, Pittsburgh, PA, USA

[3]Department of Bioengineering, University of Pittsburgh, Pittsburgh, PA, USA

Abstract

The efficacy of antidepressant treatment in late-life is modest, a problem magnified by an aging population and increased prevalence of depression. Understanding the neurobiological mechanisms of treatment response in late-life depression (LLD) is imperative. Despite established sex differences in depression and neural circuits, sex differences associated with fMRI markers of antidepressant treatment response are underexplored. In this analysis, we assess the role of sex on the relationship of acute functional connectivity changes with treatment response in LLD. Resting state fMRI scans were collected at baseline and day one of SSRI/SNRI treatment for 80 LLD participants. One-day changes in functional connectivity (differential connectivity) were related to remission status after 12 weeks. Sex differences in differential connectivity profiles that distinguished remitters from non-remitters were assessed. A random forest classifier was used to predict the remission status with models containing various combinations of demographic, clinical, symptomatological, and connectivity measures. Model performance was assessed with area under the curve, and variable importance was assessed with permutation importance. The differential connectivity profile associated with remission status differed significantly by sex. We observed evidence for a difference in one-day connectivity changes between remitters and non-remitters in males but not females. Additionally, prediction of remission was significantly improved in male-only and female-only models over pooled models. Predictions of treatment outcome based on early changes in functional connectivity show marked differences between sexes and should be considered in future MR-based treatment decision-making algorithms.

Correspondence: Carmen Andreescu, MD, 3501 Forbes Ave, Oxford Building, 530.5, Pittsburgh, PA 15213, 412-246-5698, andrcx@upmc.edu.

*Authors made equal contributions

Author Contributions: JDW developed and implemented the analytic approach and was a major contributor in writing the manuscript. ARG processed the data, guided the analytic approach, interpreted results, and was the primary contributor in writing the manuscript. HTK guided the processing, analysis, and interpretation. HJA designed the study and guided the analysis and interpretation. CA designed the study, guided analysis and interpretation, and was a major contributor in writing the manuscript.

Competing Interests: All authors declare no financial or non-financial competing interests.

1. INTRODUCTION

Major depressive disorder (MDD) is among the most common psychiatric disorders affecting almost 300 million people globally [1]. Individuals suffering from MDD have a reduced quality of life [2] and significantly increased risk of suicide [3], resulting in the third highest disability-adjusted life years of any cause and the highest among psychiatric disorders [4]. This impact is felt by people close to the afflicted individuals and across society, with an estimated economic burden of $210 billion [5]. In late-life depression (LLD), the risks are further amplified, particularly for suicide [6], comorbid cardiovascular disease [7], and cognitive impairment [8]. Additionally, treatment for LLD is only moderately effective, with multiple trials often required to find the right antidepressant medication and less than half of individuals responding to first-line treatment options [9].

Predictors or biomarkers of antidepressant treatment response have the potential to significantly reduce the burden of depression [10]. One tool that has been widely employed to investigate the neurobiological correlates of treatment response is resting state functional magnetic resonance imaging (fMRI) [11]. Measures of resting state functional connectivity (FC) are particularly fruitful for examining some of the large-scale networks [12, 13] that have been implicated in the pathophysiology of depression [14]: the default mode network (DMN), executive control network (ECN), and salience network (SN). Further, the task-free nature of resting state fMRI renders it an appealing choice for clinical application due to simplicity of acquisition and potential for generalizability [15].

Previous investigations of resting state predictors of treatment response in LLD have provided little in the way of consensus, with baseline and post-treatment FC seeded on various prefrontal and cingulate regions associated with remission [16]. Complicating the issue are apparent sex differences. It is well established that depression is nearly twice as prevalent in females than males [17], and that symptomatic profiles show marked difference between males and females [18, 19]. However, sex differences in treatment response are less conclusive, with most reporting no sex differences or better response in women [20]. Furthermore, several large studies have reported significant sex differences in resting state FC unrelated to depression [21–23]. Resting state data from the Human Connectome Project (HCP) [24] has been shown to reliably classify participants' sex with the cingulate cortex, medial and lateral frontal cortex, temporoparietal regions, insula, and precuneus (all regions important to depression and the triple network model) showing the highest discriminatory value in one study [22], and the DMN, ECN, and somatomotor networks providing the highest discriminatory value in another [23]. While the origin of these discrepancies is an open question, there is emerging evidence for various mechanisms [25–28], including genetic and endocrine pathways. Despite the apparent evidence for sex differences in neurobiology, a recent review of structural and functional MRI-based predictors of treatment outcome for depression noted only one study that reported sex differences, focused on hippocampal volume [29].

With strong evidence emerging that there are significant sex differences in the brain in general and depression specifically, there is a pressing need to investigate how sex influences the performance of MRI-derived measures of depression treatment response. While most

studies include sex as a predictor or covariate, it is unclear whether such a limited approach is sufficient to capture underlying differences. Using data from one new and one previously-analyzed study investigating neural changes predictive of remission, this analysis is believed to be the first explicit investigation of sex differences in prediction of depression treatment response with resting state fMRI. With evidence that sex differences in resting state FC become more prominent with age [21, 30], this may be particularly important for LLD.

2. METHODS

2.1. Participants

Data was collected at the University of Pittsburgh under two renewals of NIH grant R01 MH076079, Pharmacologic MRI Predictors of Treatment Response in Late-Life Depression (Circuits2, MH076079-07 through -10), and Neural Mechanisms of Monoaminergic Engagement in Late-life Depression Treatment Response (NEMO, MH076079-12 through -15). This study was approved by the University of Pittsburgh Institutional Review Board. All participants provided written informed consent prior to participating in the study.

We recruited 58 and 48 participants for Circuits2 and NEMO, respectively. Inclusion criteria were age 55 years or older (Circuits2) and 60 years or older (NEMO), diagnosis of MDD with a current major depressive episode as assessed by the Structured Clinical Interview for DSM-IV (SCID) for Circuits2 and DSM-V for NEMO (which also allowed for a diagnosis of Unspecified Depressive Disorder), Montgomery-Asberg Depression Rating Scale [31] (MADRS) greater than 15 for Circuits2 and greater than 12 for NEMO, and Mini-Mental State Exam (MMSE) score greater than 21. Exclusion criteria were history of mania or psychosis, substance abuse (current or past 3 months), dementia of any etiology, medical conditions with known significant effects on mood (e.g., stroke, current hypothyroid state), hearing/vision impairment precluding neuropsychological testing, and clinical contraindication or history of treatment resistance to venlafaxine (Circuits2) or to escitalopram and levomilnacipran (NEMO).

Circuits2 participants were treated for 12 weeks with open-label venlafaxine following a placebo lead-in, while NEMO participants were fully randomized to escitalopram or levomilnacipran for a treatment phase of 12 weeks. For both studies, the baseline visit included consent, SCID, clinical assessments and one hour of MRI. After the MRI, participants received the first dose of the medication. The second fMRI was obtained 24 hours after the first MRI, near the peak central nervous system concentration of the new medication (12-18 hours after the first oral dose of each drug). The initial doses were standardized: participants received 37.5 mg of venlafaxine, 5 mg of escitalopram, or 20 mg of levomilnacipram (initial low doses were chosen to limit potential side effects in a geriatric population). For Circuits2, venlafaxine was titrated upward weekly by 37.5 or 75 mg to reach a target dose of 150 mg/day. For NEMO, escitalopram was titrated to 10 mg escitalopram and levomilnacipram to 40 mg. Further titrations were decided by the PIs (Aizenstein/Andreescu) based on clinical response and tolerability. Seven Circuits2 participants and thirteen NEMO participants did not complete the study and were excluded from this analysis. We also excluded participants who were assigned to placebo (n = 3) as the NEMO study originally started with a placebo arm that was dropped due to low

recruitment that is common in LLD. We also excluded participants who did not complete both a baseline and day 1 scan (n = 2) and had excessive in-scanner motion (defined as >1/3 of volumes with 0.5mm or greater head jerks, n = 1). This left 51 participants in the Circuits2 cohorts and 29 participants in the NEMO cohort (see Figure 1). In both studies, participants weekly MADRS data were visually reviewed as well as a review of clinical notes to determine remission criteria.

2.2. Clinical Assessments

Basic demographic information was collected for each participant: age, sex, race, and education. Depression was assessed with the MADRS [31]. Overall anxiety was assessed with the Hamilton Anxiety Rating Scale (HARS) [32]. Additionally, disease burden was evaluated with the Cumulative Illness Rating Scale for Geriatrics (CIRS-G) [33].

2.3. Neuroimaging Acquisition

Scans for Circuits2 data were obtained on a 3T Siemens Trio TIM scanner with a standard 32 channel birdcage coil. High resolution structural images were collected with a T1-weighted magnetization-prepared rapid gradient echo (MPRAGE) sequence with the following parameters: repetition time (TR) = 2300 ms, echo time (TE = 3.4 ms), inversion time (TI) = 900 ms, flip angle = 9°, in-plane resolution of 224 x 256, 176 axial slices, and 1 mm^3 isotropic resolution. Resting state data were collected for 5 minutes with a T2*-weighted BOLD gradient-echo echoplanar sequence with the following parameters: TR = 2000 ms, TE = 34 ms, flip angle = 90°, in-plane resolution of 128 x 128, 28 axial slices, and 2 x 2 x 4 mm resolution. Scans for NEMO data were obtained on a 3T Siemens Prisma FIT scanner with a standard 64 channel birdcage coil for 15 participants and a 7T Siemens Magnetom scanner using a customized 16/32-channel transmit/receive (respectively) head coil [34] for 24 participants. High resolution structural images were collected on both scanners with a T1-weighted MPRAGE sequence. The parameters for the 3T scan were: TR = 3000 ms, TE = 2.3 ms, TI = 1000 ms, flip angle = 8°, in-plane resolution of 300 x 320, 280 sagittal slices, 0.8 mm^3 isotropic resolution, and Generalized Autocalibrating Partial Parallel Acquisition (GRAPPA) acceleration factor of 2. The parameters for the 7T scan were: TR = 3000 ms, TE = 2.3 ms, TI = 1200 ms, flip angle = 8°, in-plane resolution of 230 x 320, 256 axial slices, 0.75 mm^3 isotropic resolution, and GRAPPA acceleration factor of 2. Resting state data were collected for 6 minutes with a T2*-weighted BOLD echoplanar imaging sequence. The parameters for the 3T scan were: TR = 1000 ms, TE = 30 ms, flip angle = 45°, in-plane resolution of 96 x 96, 60 axial slices, 2.3 mm^3 isotropic resolution, and multiband acceleration factor of 5. The parameters for the 7T scan were: TR = 1000 ms, TE = 20 ms, flip angle = 65°, in-plane resolution of 110 x 110, 60 axial slices, 2 mm^3 isotropic resolution, and multiband acceleration factor of 3. All scans were conducted at the Magnetic Resonance Research Center at the University of Pittsburgh.

2.4. Image Preprocessing

All MRI preprocessing was performed using the Statistical Parametric Mapping (SPM12) toolbox [35] in Matlab unless otherwise noted. Structural images were segmented into six tissue types based on spatial priors, which generated deformation fields to standard Montreal Neurological Institute (MNI) space for each subject. Two Gaussians were used

to identify white matter, which provides better grey/white matter differentiation in older adults where white matter hyperintensity burden can be high [36]. For the functional images, slice-time correction and motion correction were applied before skull-stripping with the brain extraction tool [37] from the FMRIB Software Library. The skull-stripped images were then co-registered to the structural image using normalized mutual information, normalized to MNI space, and smoothed using a Gaussian kernel with full-width half-maximum of 8 mm. The BrainWavelet toolbox [38] was used to remove motion-induced spike artifacts. The six rigid-body motion parameters (translation and rotation in each direction), the first five principal components of the white matter and cerebral spinal fluid signal, and frequencies outside the resting state band of 0.008 to 0.15 Hz were simultaneously regressed out of the signal to avoid reintroducing artifacts [39].

2.5 Functional Connectivity Calculation

Mean residual time series were then calculated for each region in the Shen 50 atlas [40]. This functionally-derived parcellation provides an optimal balance between specificity and parsimony for this application. Functional connectivity was calculated using pairwise Pearson correlation between region time series for each participant. We removed regions labelled 1, 3, 13, 38, 43, 53, 54, 61, 84, 88, and 89 from the atlas due to poor coverage in the cerebellum, resulting in 3,321 unique pairwise connections among the 82 remaining regions.

Functional connectivity matrices from all 80 participants in the analysis were harmonized to account for batch effects from scanner (3T Siemens Prisma FIT or 7T Siemens Magnetom) and study (Circuits2 or NEMO) while preserving the variability explained by sex and age using the ComBat empirical Bayes' method [41] adjusted for functional connectivity harmonization [42]. Implementation of ComBat was performed using the neuroCombat package in R using publicly available code.

Differential connectivity was calculated as the difference in harmonized functional connectivity on day 1 (approximately 1 day after first antidepressant dose) and functional connectivity at baseline for each of the 3,321 pairwise connections.

2.6. Statistical Analyses

Two sample *t*-tests and chi-squared tests were used to compare means and proportions, respectively, for demographic and other participant characteristics. An illustrative flow chart describing all other statistical analyses performed in this study is provided in Figure 2; details of the analyses are provided below. The power analysis for the NEMO study estimated data from 80 participants was required to achieve a power of 0.8 at the 0.05 significance level. We therefore elected to augment the ongoing NEMO data with Circuits2 data to obtain adequate power for this midterm analysis. For all analyses, we verified that the appropriate statistical assumptions were met for the methods employed.

2.5.1. Remitter Differences—The average differential connectivity for each pair of regions was calculated for the remitter and non-remitter groups according to sex, and differences were evaluated using two-sample *t*-tests. Given the large number of region-pairs and lack of an established multiple comparisons correction method that can account for

the high level of correlation among the tests, we did not perform multiple comparisons correction and avoid inference on individual edges, instead focusing on broad region-wise summaries of connectivity differences between the sexes. To calculate region-wise values, we set all t values for pairwise connections with uncorrected $p < .05$ to zero and then average across all the t values for all 81 pairwise connections to each region. Additionally, we used Higher Criticism [43, 44] to perform an omnibus test for a global differential connectivity difference between remitters and non-remitters in males and females separately. The Higher Criticism statistic compares the distribution of p-values from a large family of tests to the null (uniform) distribution to test for a global difference. This method is optimal in the rare and weak regime, though it can only detect a deviation in the body of tests, not which tests differ significantly. Given the large number of tests (3,321 in this case), the resulting statistic asymptotically approaches a one-sided z statistic.

2.5.2. Prediction of Remission with Functional Connectivity—Next, we implemented a machine learning approach to predict the remission status of each participant, where remission is a binary outcome indicating whether a participant had a final MADRS score of 10 or less for at least 2 weeks, subject to clinical judgment by the study psychiatrist who was blinded to the analysis. Random forest models were used to predict remission based on features describing (1) demographic confounders including age, sex, race, and education level, (2) clinical data including scanner (3T or 7T) and the CIRS-G, (3) baseline depression severity measured by MADRS and anxiety severity measured by the HARS, (4) baseline functional connectivity, and (5) differential connectivity. Random forest models were fit using the *RandomForest* function in R [45] and run with default parameter settings with $m = 500$ trees and $p = 2/3$ of the independent variables provided in the model. Splits in each decision tree were decided using the Gini index criterion [46]. Seven different random forest models were fit with a unique set of predictor variables, labeled A-G as provided in Table 1. Model performance was assessed by predictive area under the curve (AUC) calculated over 30 repetitions with random 90%/10% training/test splits. Data splits were consistent across all models, ensuring that each model was trained and tested on the same data. Within the training sample, Monte Carlo cross validation was employed using randomly selected samples with random training size sampled uniformly between 50% and 80%. AUC values were compared across male-only, female-only, and pooled models using two-sample t-tests over the out-of-sample results of the 30 repetitions.

2.5.3. Variable Importance—For the random forest model containing all clinical, demographic and depression symptomatology, and differential connectivity measures (model F), the permutation importance (mean decrease in out-of-sample classification error over all splits) of each variable was calculated using the VarImpPlot function in R. Region-wise averages of variable importance are provided in Figure 3. Brain image plots were created using BrainNet Viewer software [47] in Matlab v. R2020b. All R software was implemented using R version 1.4.1717.

3. RESULTS

Table 2 and Supplementary Tables 1 and 2 summarize the combined and separate clinical and demographic information for the participants in the NEMO and Circuits2 cohorts that

were analyzed in this study. Among demographic and clinical variables, only the number of participants differed significantly by sex, which is consistent with greater prevalence of depression among females. The characteristics of the two studies were similar and no significant differences were noted aside from medications, which differed by study design, and the ratio of males to females enrolled in the Circuits2 study.

3.1. Differential Connectivity Differences between Remitters and Non-Remitters Depend on Sex

We first compared the one-day differential connectivity between remitters and non-remitters to evaluate the extent to which connections differ between the two groups. The resulting positive and negative *t*-statistics were averaged separately across all connections for each region; regional summaries are shown in Figure 3.

For males, the remitter group was associated with increased connectivity from baseline to day 1 for the right caudate, left middle temporal pole, and left postcentral gyrus and by decreased connectivity from baseline to day 1 for the left caudate, left putamen, and right middle temporal gyrus. The Higher Criticism statistic for the edge-wise group of *t*-tests was $z = 4.33$, ($p < 0.001$), indicating statistically significant evidence for a global differential connectivity signature distinguishing male remitters from non-remitters.

For females, the remitter status group was associated with increased connectivity from baseline to day 1 for the left thalamus, dorsal anterior cingulate, and precentral gyrus and by decreased connectivity from baseline to day 1 for the left dorsomedial prefrontal cortex and right angular gyrus. The Higher Criticism statistic for the edge-wise group of *t*-tests was $z = -3.11$, ($p = 0.999$), indicating no evidence for a global differential connectivity signature distinguishing female remitters from non-remitters.

3.2. The Predictive Relationship between Functional Connectivity and Remission is Moderated by Sex

The mean and standard deviation of the AUCs obtained from each of the seven models described in Table 1 are shown in Figure 4 and Supplementary Table 3. In all but one of the seven considered models, at last one of the models fitted separately for males or females significantly outperforms the average performance of the predictive models containing both males and females. For four models each, the predictive AUCs of the male-only and female-only models are significantly greater than the AUC of the pooled model. Notably, the only model in which the male-only or female-only models did not outperform the pooled model is model E, which does not use differential connectivity as a predictor. Taken together, pooled models obtained an average AUC of 0.69 whereas female-only models achieved an average AUC of 0.74 and male-only models achieved an average AUC of 0.76, providing an improvement in predictive AUCs of 7% and 10%, respectively. We repeated this same analysis on each cohort separately and found consistent results across both cohorts. For the Circuits2 cohort, we found a mean improvement of 13% for female-only models (mean AUC = 0.794) and an improvement of 42% (mean AUC = 0.981) for male-only models over the pooled models (mean AUC = 0.704). In the NEMO cohort, we found a mean

improvement of 15% for both male- and female-only models (mean AUC = 0.987, 0.989, respectively) over pooled models (mean AUC = 0.857).

For model F (demographic, clinical, depression symptomatology, and differential connectivity predictors) the regional average of permutation importance of each edge is shown in Figure 5 for the male-only model, female-only model, and the normalized difference between the two. Of the non-imaging variables in each fitted model, only depression symptomatology had a non-zero variable importance, and this was only in the female-only model (variable importance = 0.008).

For males, the changes in connectivity for the left caudate, left middle temporal pole, and left orbital frontal gyrus were the most important in predicting remission (see Fig 5, Table 3). For females, the changes in connectivity for the left caudate, left paracentral lobule, and left lingual (medial occipito-temporal) gyrus were the most important in predicting remission.

4. DISCUSSION

Our study shows that one day changes in resting state functional indicators of treatment response in late-life depression are sex-dependent. This result was consistent in both explanatory and predictive frameworks. Acute one-day changes in functional connectivity among remitter and non-remitter groups greatly differed between males and females. Further, there was strong evidence from the higher criticism test for an omnibus differential connectivity signature differentiating remitters from non-remitters in males, but not females. By separating the predictive analyses into male- and female-only cohorts, we obtained an average increase of 7 - 40% in predictive AUC across models containing clinical, demographic, depression symptomatology, baseline functional connectivity, and one-day change in connectivity. Additionally, male-only models provided the greatest performance increase. In our study of 80 participants from two separate cohorts, we found that male-only models were always significantly better at prediction than pooled models containing both male and female participants.

Additionally, male-only models typically performed better than female-only models. This is unsurprising given the more robust differential connectivity differences in remitters vs. non-remitters for males compared to females, but comparison of the regions important in the explanatory and predictive frameworks reveals an interesting dichotomy. The regions with the highest average variable importance for the male predictive models are also the regions showing the greatest differences between male remitters and non-remitters, as would be expected. However, this is not the case for females. In fact, the most important region in the female predictive model (the left caudate) shows a relatively minor difference between remitters and non-remitters. This also manifests in greater variable importances for the female predictive model compared to the male model. While this may seem counterintuitive, this may be an effect of “easier” prediction in males by keying on regions that differ significantly between remitters and non-remitter while the lack of such differences in females requires the predictive model to rely on more complex patterns.

We also showed that males and females recruit different nodes in the early stages of successful treatment. In males, early disengagement of the left striatum and right temporal/insular complex and early engagement of left postcentral and lingual gyri and right caudate nucleus were associated with remission, while in females there is no strong evidence for functional connectivity changes that distinguish remitters from non-remitters. Our results point toward a sex-specific dynamic profile in the engagement and disengagement of key regions during pharmacotherapy. We also report that the connectivity indices relevant for predicting remission are primarily different between the two sexes: left caudate for both sexes, left temporal pole, left orbitofrontal cortex, and right dorsomedial prefrontal cortex (PFC) for males; left paracentral lobule, left lingual gyrus, and bilateral superior parietal lobes for females.

LLD remission has previously been associated with lower baseline FC between the PCC and left striatum [48] and higher baseline FC between the right and left dlPFC, left dlPFC and dorsal anterior cingulate cortex (ACC), and right dlPFC and right inferior parietal lobe, but not with baseline FC within the DMN [49]. Longitudinal studies have reported remission to be associated with 12-week increases in FC between the PCC and the bilateral inferior and middle temporal gyri (using Circuits 2 data) [50], precentral gyrus [48] and subgenual ACC/dorsomedial PFC [51]. All these results employed a priori seeds to analyze FC. Considering only differential connectivity edges that showed a significant difference between remitters and non-remitters (uncorrected) and a non-zero variable importance in the predictive model, our whole-brain analysis also identified increased connectivity between the PCC and the precentral gyrus for both males and females; dlPFC, dorsomedial PFC, and MTG/angular gyrus for females; and subgenual ACC/orbitofrontal cortex for males. However, the PCC did not stand out as a major differentiator of remitters, in either the traditional associative tests or predictive model. This adds to growing evidence that interactions between the canonical networks may be more important than DMN-specific connectivity [52, 53].

While no studies were found examining sex differences in resting state functional connectivity in LLD, there is a wealth of research in healthy populations. HCP data has been combined with 1,000 functional connectomes data [54] to show that sex-differences in hierarchical modularity emerge with increasing age, particularly in the prefrontal cortex, temporal lobe, amygdala, hippocampus, inferior parietal lobe, posterior cingulate, and precuneus [30]. Resting state sex differences were also reported in the 1000 functional connectomes data across methodologies (seed-based connectivity, independent component analysis (ICA), and amplitude of low frequency fluctuation) [54], though important regions were not explicitly reported. ICA has also been used to demonstrate that females generally show stronger intra-network connectivity, while males show stronger inter-network connectivity, especially in the somatomotor network, as well as decreasing network coherence and connectivity with age [55]. This finding of stronger intra-network connectivity for females and stronger inter-network connectivity in males has also been reported in a large study of adolescents across a wider array of networks including the DMN, ventral attention network, auditory network, and memory retrieval network [56]. Using the UK Biobank data, greater connectivity within the DMN of older females and greater connectivity within the sensorimotor cortices in older males has also been reported [21]. Studies investigating the hemispheric organizational patterns of resting state FC

identified sex differences in the developmental trajectory across the lifespan within the dlPFC and amygdala [57] as well as higher clustering attributes in the right hemisphere in males and left hemisphere in females [58]. Meanwhile, two smaller, older studies reported no sex differences in resting state FC [59, 60].

Recent studies, including Circuits2, have demonstrated the feasibility of acute trajectories of functional connectivity to predict remission in late-life depression [16, 50, 61]. Our study takes advantage of the serial imaging acquisition embedded in the design of these studies, which allowed us to test treatment prediction using one day acute dynamic changes in functional connectivity. With a few notable exceptions [50, 62, 63], most studies investigating FC signatures of remission rely on baseline FC measures or FC changes over the treatment course. The one-day change paradigm may offer 1) an early indication of treatment response that could be used to augment clinical judgment and 2) a significant advantage over baseline measures by capturing antidepressant-induced changes in intrinsic brain activity. This replicates our prior results that the pharmacologic probe (pre versus post medication) is predictive of remission [50, 61]. The results, while highlighting regions and networks frequently described in LLD [52, 53], indicate that analyses that combine the two sexes may not be representative for each sex.

Remission in women implicates an increase in connectivity of the ACC and thalamus and a disengagement of frontal regions and the insular cortex together with temporo-parietal regions, while remission in men implicates increased connectivity in posterior regions and a disengagement of the striatum and middle temporal gyrus. The anterior cingulate engagement and insular disengagement in females coupled with the double remission rate observed in women in this sample may suggest that Salience Network dynamics are key for remission in women. Interestingly, the male-specific profile is centered mostly on the striatum and temporo-parietal nodes and male-specific models are more accurate than female or global models in predicting remission. These results suggest that the networks dynamic tilts toward an Executive Control/Reward interplay as a remission marker in men. Given the large body of literature exploring reward circuitry and the striatum in midlife depression, it is surprising how few studies have done the same in LLD [64]. Based on our study, we posit that splitting prediction based on sex is a necessary step toward single-subject prediction modeling.

Equally significant, the random forest algorithm adds another layer of complexity that indicates that the nodes that engage/disengage the most early in the treatment are not necessarily the stronger predictors of treatment remission. The regions important in both the explanatory and predictive frameworks were generally overlapping for males, but not females. This may indicate that both reactivity to antidepressants and consequences of those changes are discrepant between the sexes. Key regions relevant for treatment prediction are also different in men and women. However, for both sexes, the strongest predictor for treatment remission was the left caudate connectivity (including the left nucleus accumbens), a key reward network region implicated in depression [65–67]. We speculate that the early engagement of the ventral striatum/accumbens may trigger downstream cascades engaging projections to ventral pallidum-dorsal thalamus-prefrontal cortex but also

projections to the reticular formation and ventral tegmental area, changes which ultimately translate in clinical improvement.

Our study has several limitations including a moderate sample size, the use of multiple antidepressants, lack of placebo, imaging done at both 3T and 7T, short resting state acquisition for Circuits2, variable importance quantification, and lack of validation sample. The moderate sample size limits our ability to perform inference on individual region-pair changes in functional connectivity [68]. Further, small sample sizes may inflate accuracy estimation in predictive models. The use of multiple antidepressants introduces additional heterogeneity, though this may increase the generalizability of our findings. The lack of a placebo arm limits our ability to interpret the changes as specifically induced by antidepressants. While placebo arms can be considered in future studies, they may raise ethical challenges in studies of difficult-to-treat depression. This may also apply to the use of two scanner types. The short duration for the Circuits2 resting state acquisition limits the robustness of the connectivity measures [69]. In the last decade, there has been substantial discussion about the suitability of variable importance measures in machine learning models [70]. In our study, we chose to quantify differential connectivity variable importance using permutation importance because the ease of interpretability and generalizability [71, 72]. This broad applicability allows for direct comparisons of our present study to other possible statistical and machine learning methods like neural networks and logistic regression, though it may be subject to bias. The cross-validation utilized a nested approach without a true validation sample (completely unseen dataset) which likely inflates the overall accuracies but was necessary given the small sample size. It is unclear how much these generalize or other drugs or therapies in LLD as well as to depression in midlife or adolescence. However, given the evidence for sex differences in resting state FC, the general conclusion that the effect of sex cannot be accounted for simply by including it as a predictor seems likely to be true across the lifespan.

In conclusion, we present novel data indicating the essential role of sex differences in predicting treatment response in late-life depression using resting state connectivity data. The results of our study add a key step toward incorporating prediction models in the clinical decision-making process.

Supplementary Material

Refer to Web version on PubMed Central for supplementary material.

Acknowledgements:

This study was funded by NIMH grants R01 MH076079, R01 MH108509, R01 MH121619, K01 MH122741, and T32 MH019986. The funder played no role in study design, data collection, analysis and interpretation of data, or the writing of this manuscript.

Data/Code Availability:

The datasets and code used and/or analyzed during the current study available from the corresponding author on reasonable request.

REFERENCES

1. Whiteford HA, Ferrari AJ, Degenhardt L, Feigin V, Vos T. The global burden of mental, neurological and substance use disorders: an analysis from the Global Burden of Disease Study 2010. PloS One. 2015;10:e0116820. [PubMed: 25658103]
2. Brenes GA. Anxiety, Depression, and Quality of Life in Primary Care Patients. Prim Care Companion J Clin Psychiatry. 2007;9:437–443. [PubMed: 18185823]
3. Strakowski S, Nelson E. Major Depressive Disorder. Oxford University Press; 2015.
4. Murray CJL, Vos T, Lozano R, Naghavi M, Flaxman AD, Michaud C, et al. Disability-adjusted life years (DALYs) for 291 diseases and injuries in 21 regions, 1990–2010: a systematic analysis for the Global Burden of Disease Study 2010. The Lancet. 2012;380:2197–2223.
5. Greenberg PE, Fournier A-A, Sisitsky T, Pike CT, Kessler RC. The economic burden of adults with major depressive disorder in the United States (2005 and 2010). J Clin Psychiatry. 2015;76:155–162. [PubMed: 25742202]
6. Conwell Y, Van Orden K, Caine ED. Suicide in Older Adults. Psychiatr Clin North Am. 2011;34:451–468. [PubMed: 21536168]
7. Wei J, Lu Y, Li K, Goodman M, Xu H. The associations of late-life depression with all-cause and cardiovascular mortality: The NHANES 2005–2014. J Affect Disord. 2022;300:189–194. [PubMed: 34971700]
8. Ganguli M, Du Y, Dodge HH, Ratcliff GG, Chang C-CH. Depressive Symptoms and Cognitive Decline in Late Life: A Prospective Epidemiological Study. Arch Gen Psychiatry. 2006;63:153–160. [PubMed: 16461857]
9. Trivedi MH, Rush AJ, Wisniewski SR, Nierenberg AA, Warden D, Ritz L, et al. Evaluation of Outcomes With Citalopram for Depression Using Measurement-Based Care in STAR*D: Implications for Clinical Practice. Am J Psychiatry. 2006;163:28–40. [PubMed: 16390886]
10. Thase ME. Using biomarkers to predict treatment response in major depressive disorder: evidence from past and present studies. Dialogues Clin Neurosci. 2014;16:539–544. [PubMed: 25733957]
11. Dichter GS, Gibbs D, Smoski MJ. A systematic review of relations between resting-state functional-MRI and treatment response in major depressive disorder. J Affect Disord. 2015;172:8–17. [PubMed: 25451389]
12. Damoiseaux JS, Rombouts SARB, Barkhof F, Scheltens P, Stam CJ, Smith SM, et al. Consistent resting-state networks across healthy subjects. Proc Natl Acad Sci U S A. 2006;103:13848–13853. [PubMed: 16945915]
13. Smith SM, Fox PT, Miller KL, Glahn DC, Fox PM, Mackay CE, et al. Correspondence of the brain's functional architecture during activation and rest. Proc Natl Acad Sci. 2009;106:13040–13045. [PubMed: 19620724]
14. Menon V. Large-scale brain networks and psychopathology: a unifying triple network model. Trends Cogn Sci. 2011;15:483–506. [PubMed: 21908230]
15. Fox MD, Greicius M. Clinical Applications of Resting State Functional Connectivity. Front Syst Neurosci. 2010;4:19. [PubMed: 20592951]
16. Dunlop K, Talishinsky A, Liston C. Intrinsic Brain Network Biomarkers of Antidepressant Response: a Review. Curr Psychiatry Rep. 2019;21:87. [PubMed: 31410661]
17. Salk RH, Hyde JS, Abramson LY. Gender differences in depression in representative national samples: Meta-analyses of diagnoses and symptoms. Psychol Bull. 2017;143:783–822. [PubMed: 28447828]
18. Eid RS, Gobinath AR, Galea LAM. Sex differences in depression: Insights from clinical and preclinical studies. Prog Neurobiol. 2019;176:86–102. [PubMed: 30721749]
19. Silverstein B, Edwards T, Gamma A, Ajdacic-Gross V, Rossler W, Angst J. The role played by depression associated with somatic symptomatology in accounting for the gender difference in the prevalence of depression. Soc Psychiatry Psychiatr Epidemiol. 2013;48:257–263. [PubMed: 22752109]
20. Einstein G, Downar J, Kennedy SH. Gender/sex differences in emotions. Medicographia. 2013;35:271–280.

21. Ritchie SJ, Cox SR, Shen X, Lombardo MV, Reus LM, Alloza C, et al. Sex Differences in the Adult Human Brain: Evidence from 5216 UK Biobank Participants. Cereb Cortex. 2018;28:2959–2975. [PubMed: 29771288]
22. Weis S, Patil KR, Hoffstaedter F, Nostro A, Yeo BTT, Eickhoff SB. Sex Classification by Resting State Brain Connectivity. Cereb Cortex. 2020;30:824–835. [PubMed: 31251328]
23. Zhang C, Dougherty CC, Baum SA, White T, Michael AM. Functional connectivity predicts gender: Evidence for gender differences in resting brain connectivity. Hum Brain Mapp. 2018;39:1765–1776. [PubMed: 29322586]
24. Van Essen DC, Ugurbil K, Auerbach E, Barch D, Behrens TEJ, Bucholz R, et al. The Human Connectome Project: A data acquisition perspective. NeuroImage. 2012;62:2222–2231. [PubMed: 22366334]
25. Rubinow DR, Schmidt PJ. Sex differences and the neurobiology of affective disorders. Neuropsychopharmacology. 2019;44:111–128. [PubMed: 30061743]
26. Seney ML, Sibille E. Sex differences in mood disorders: perspectives from humans and rodent models. Biol Sex Differ. 2014;5:17. [PubMed: 25520774]
27. Bangasser DA, Cuarenta A. Sex differences in anxiety and depression: circuits and mechanisms. Nat Rev Neurosci. 2021;22:674–684. [PubMed: 34545241]
28. Talishinsky A, Downar J, Vértes PE, Seidlitz J, Dunlop K, Lynch CJ, et al. Regional gene expression signatures are associated with sex-specific functional connectivity changes in depression. Nat Commun. 2022;13:5692. [PubMed: 36171190]
29. Vakili K, Pillay SS, Lafer B, Fava M, Renshaw PF, Bonello-Cintron CM, et al. Hippocampal volume in primary unipolar major depression: a magnetic resonance imaging study. Biol Psychiatry. 2000;47:1087–1090. [PubMed: 10862809]
30. Conrin SD, Zhan L, Morrissey ZD, Xing M, Forbes A, Maki P, et al. From Default Mode Network to the Basal Configuration: Sex Differences in the Resting-State Brain Connectivity as a Function of Age and Their Clinical Correlates. Front Psychiatry. 2018;9. [PubMed: 29445345]
31. Montgomery SA, Asberg M. A new depression scale designed to be sensitive to change. Br J Psychiatry J Ment Sci. 1979;134:382–389.
32. Hamilton M. The assessment of anxiety states by rating. Br J Med Psychol. 1959;32:50–55. [PubMed: 13638508]
33. Miller MD, Paradis CF, Houck PR, Mazumdar S, Stack JA, Rifai AH, et al. Rating chronic medical illness burden in geropsychiatric practice and research: application of the Cumulative Illness Rating Scale. Psychiatry Res. 1992;41:237–248. [PubMed: 1594710]
34. Ibrahim TS, Zhao Y, Krishnamurthy N, Raval S, Zhao T, Wood S, et al. 20-To-8 channel Tx array with 32-channel adjustable receive-only insert for 7T head imaging2013. p. 4408.
35. Penny WD, Friston KJ, Ashburner JT, Kiebel SJ, Nichols TE. Statistical parametric mapping: the analysis of functional brain images. Elsevier; 2011.
36. Karim HT, Andreescu C, MacCloud RL, Butters MA, Reynolds CF 3rd, Aizenstein HJ, et al. The effects of white matter disease on the accuracy of automated segmentation. Psychiatry Res Neuroimaging. 2016;253:7–14. [PubMed: 27254085]
37. Smith SM. Fast robust automated brain extraction. Hum Brain Mapp. 2002;17:143–155. [PubMed: 12391568]
38. Patel AX, Kundu P, Rubinov M, Jones PS, Vértes PE, Ersche KD, et al. A wavelet method for modeling and despiking motion artifacts from resting-state fMRI time series. Neuroimage. 2014;95:287–304. [PubMed: 24657353]
39. Lindquist MA, Geuter S, Wager TD, Caffo BS. Modular preprocessing pipelines can reintroduce artifacts into fMRI data. Hum Brain Mapp. 2019;40:2358–2376. [PubMed: 30666750]
40. Shen X, Tokoglu F, Papademetris X, Constable RT. Groupwise whole-brain parcellation from resting-state fMRI data for network node identification. NeuroImage. 2013;82:403–415. [PubMed: 23747961]
41. Johnson WE, Li C, Rabinovic A. Adjusting batch effects in microarray expression data using empirical Bayes methods. Biostatistics. 2007;8:118–127. [PubMed: 16632515]

42. Yu M, Linn KA, Cook PA, Phillips ML, McInnis M, Fava M, et al. Statistical harmonization corrects site effects in functional connectivity measurements from multi-site fMRI data. Hum Brain Mapp. 2018;39:4213–4227. [PubMed: 29962049]
43. Donoho D, Jin J. Higher criticism for detecting sparse heterogeneous mixtures. Ann Stat. 2004;32:962–994.
44. Donoho D, Jin J. Higher Criticism for Large-Scale Inference, Especially for Rare and Weak Effects. Stat Sci. 2015;30:1–25.
45. R Core Team. R: A Language and Environment for Statistical Computing. Vienna, Austria: R Foundation for Statistical Computing; 2021.
46. Breiman L Random Forests. Mach Learn. 2001;45:5–32.
47. Xia M, Wang J, He Y. BrainNet Viewer: A Network Visualization Tool for Human Brain Connectomics. PLOS ONE. 2013;8:e68910. [PubMed: 23861951]
48. Andreescu C, Tudorascu DL, Butters MA, Tamburo E, Patel M, Price J, et al. Resting state functional connectivity and treatment response in late-life depression. Psychiatry Res. 2013;214:10.1016/j.pscychresns.2013.08.007.
49. Alexopoulos GS, Hoptman MJ, Kanellopoulos D, Murphy CF, Lim KO, Gunning FM. Functional connectivity in the cognitive control network and the default mode network in late-life depression. J Affect Disord. 2012;139:56–65. [PubMed: 22425432]
50. Karim HT, Andreescu C, Tudorascu D, Smagula SF, Butters MA, Karp JF, et al. Intrinsic functional connectivity in late-life depression: trajectories over the course of pharmacotherapy in remitters and non-remitters. Mol Psychiatry. 2017;22:450–457. [PubMed: 27090303]
51. Wu M, Andreescu C, Butters MA, Tamburo R, Reynolds CF, Aizenstein H. Default-mode network connectivity and white matter burden in late-life depression. Psychiatry Res Neuroimaging. 2011;194:39–46.
52. Gunning FM, Oberlin LE, Schier M, Victoria LW. Brain-based mechanisms of late-life depression: Implications for novel interventions. Semin Cell Dev Biol. 2021;116:169–179. [PubMed: 33992530]
53. Gerlach AR, Karim HT, Peciña M, Ajilore O, Taylor WD, Butters MA, et al. MRI predictors of pharmacotherapy response in major depressive disorder. NeuroImage Clin. 2022;36:103157. [PubMed: 36027717]
54. Biswal BB, Mennes M, Zuo X-N, Gohel S, Kelly C, Smith SM, et al. Toward discovery science of human brain function. Proc Natl Acad Sci U S A. 2010;107:4734–4739. [PubMed: 20176931]
55. Allen EA, Erhardt EB, Damaraju E, Gruner W, Segall JM, Silva RF, et al. A Baseline for the Multivariate Comparison of Resting-State Networks. Front Syst Neurosci. 2011;5:2. [PubMed: 21442040]
56. Satterthwaite TD, Wolf DH, Roalf DR, Ruparel K, Erus G, Vandekar S, et al. Linked Sex Differences in Cognition and Functional Connectivity in Youth. Cereb Cortex. 2015;25:2383–2394. [PubMed: 24646613]
57. Zuo X-N, Kelly C, Di Martino A, Mennes M, Margulies DS, Bangaru S, et al. Growing Together and Growing Apart: Regional and Sex Differences in the Lifespan Developmental Trajectories of Functional Homotopy. J Neurosci. 2010;30:15034–15043. [PubMed: 21068309]
58. Tian L, Wang J, Yan C, He Y. Hemisphere- and gender-related differences in small-world brain networks: a resting-state functional MRI study. NeuroImage. 2011;54:191–202. [PubMed: 20688177]
59. Bluhm RL, Osuch EA, Lanius RA, Boksman K, Neufeld RWJ, Théberge J, et al. Default mode network connectivity: effects of age, sex, and analytic approach. Neuroreport. 2008;19:887–891. [PubMed: 18463507]
60. Weissman-Fogel I, Moayedi M, Taylor KS, Pope G, Davis KD. Cognitive and default-mode resting state networks: do male and female brains 'rest' differently? Hum Brain Mapp. 2010;31:1713–1726. [PubMed: 20725910]
61. Karim HT, Wang M, Andreescu C, Tudorascu D, Butters MA, Karp JF, et al. Acute trajectories of neural activation predict remission to pharmacotherapy in late-life depression. NeuroImage Clin. 2018;19:831–839. [PubMed: 30013927]

62. Fu CHY, Costafreda SG, Sankar A, Adams TM, Rasenick MM, Liu P, et al. Multimodal functional and structural neuroimaging investigation of major depressive disorder following treatment with duloxetine. BMC Psychiatry. 2015;15:82. [PubMed: 25880400]

63. Nemati S, Akiki TJ, Roscoe J, Ju Y, Averill CL, Fouda S, et al. A Unique Brain Connectome Fingerprint Predates and Predicts Response to Antidepressants. IScience. 2019;23:100800. [PubMed: 31918047]

64. Taylor WD, Zald DH, Felger JC, Christman S, Claassen DO, Horga G, et al. Influences of dopaminergic system dysfunction on late-life depression. Mol Psychiatry. 2021. 17 August 2021. 10.1038/s41380-021-01265-0.

65. Keren H, O'Callaghan G, Vidal-Ribas P, Buzzell GA, Brotman MA, Leibenluft E, et al. Reward Processing in Depression: A Conceptual and Meta-Analytic Review Across fMRI and EEG Studies. Am J Psychiatry. 2018;175:1111–1120. [PubMed: 29921146]

66. Steffens DC, Krishnan KRR. Structural neuroimaging and mood disorders: Recent findings, implications for classification, and future directions. Biol Psychiatry. 1998;43:705–712. [PubMed: 9606523]

67. Lorenzetti V, Allen NB, Fornito A, Yücel M. Structural brain abnormalities in major depressive disorder: A selective review of recent MRI studies. J Affect Disord. 2009;117:1–17. [PubMed: 19237202]

68. Button KS, Ioannidis JPA, Mokrysz C, Nosek BA, Flint J, Robinson ESJ, et al. Power failure: why small sample size undermines the reliability of neuroscience. Nat Rev Neurosci. 2013;14:365–376. [PubMed: 23571845]

69. Birn RM, Molloy EK, Patriat R, Parker T, Meier TB, Kirk GR, et al. The effect of scan length on the reliability of resting-state fMRI connectivity estimates. NeuroImage. 2013;83:550–558. [PubMed: 23747458]

70. Strobl C, Boulesteix A-L, Zeileis A, Hothorn T. Bias in random forest variable importance measures: Illustrations, sources and a solution. BMC Bioinformatics. 2007;8:25. [PubMed: 17254353]

71. Sundararajan M, Najmi A. The Many Shapley Values for Model Explanation. Proc. 37th Int. Conf. Mach. Learn., PMLR; 2020. p. 9269–9278.

72. Parr T, Wilson JD. Partial dependence through stratification. Mach Learn Appl. 2021;6:100146.

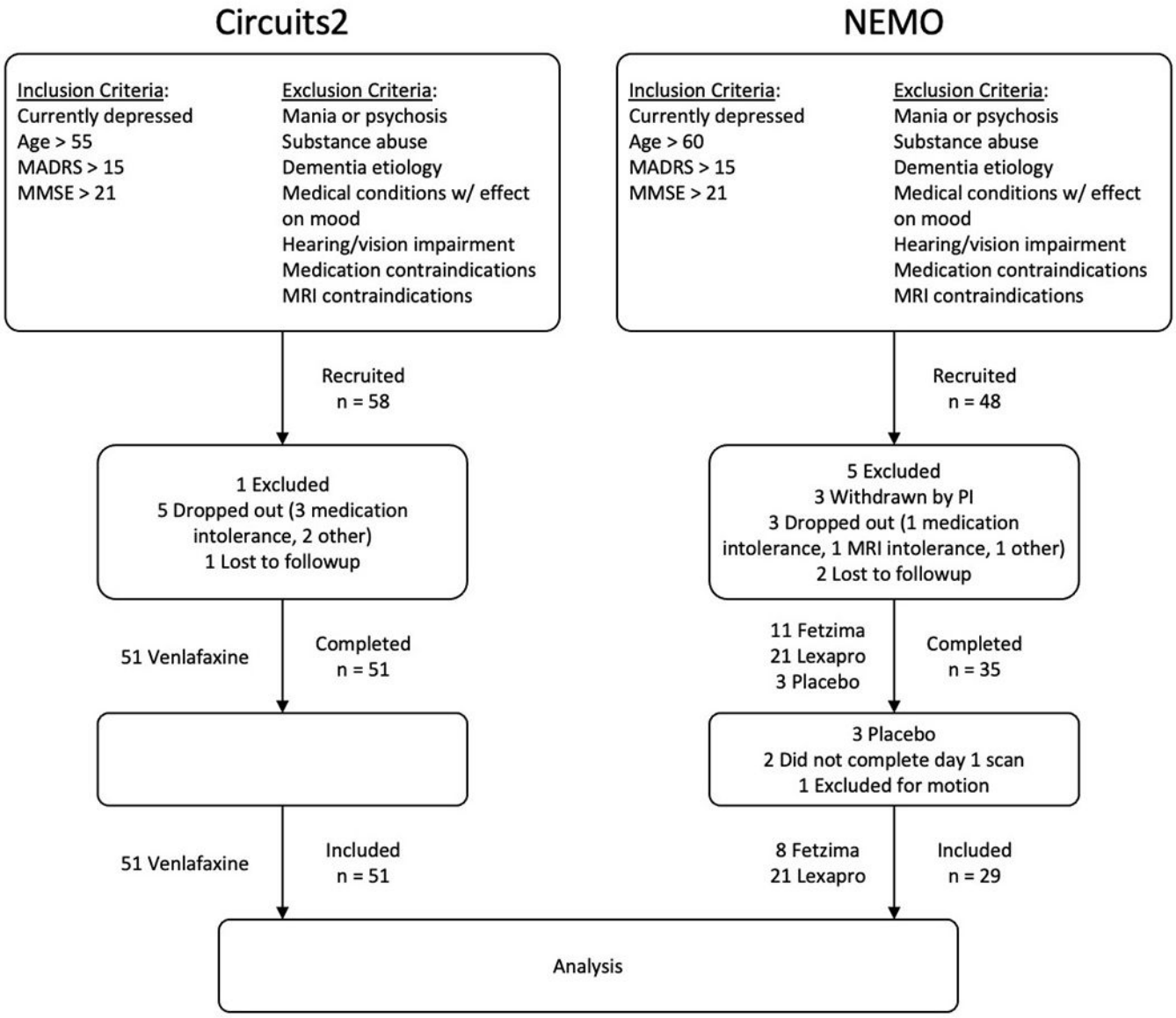

Figure 1.
CONSORT diagrams for the Circuits2 and NEMO studies.

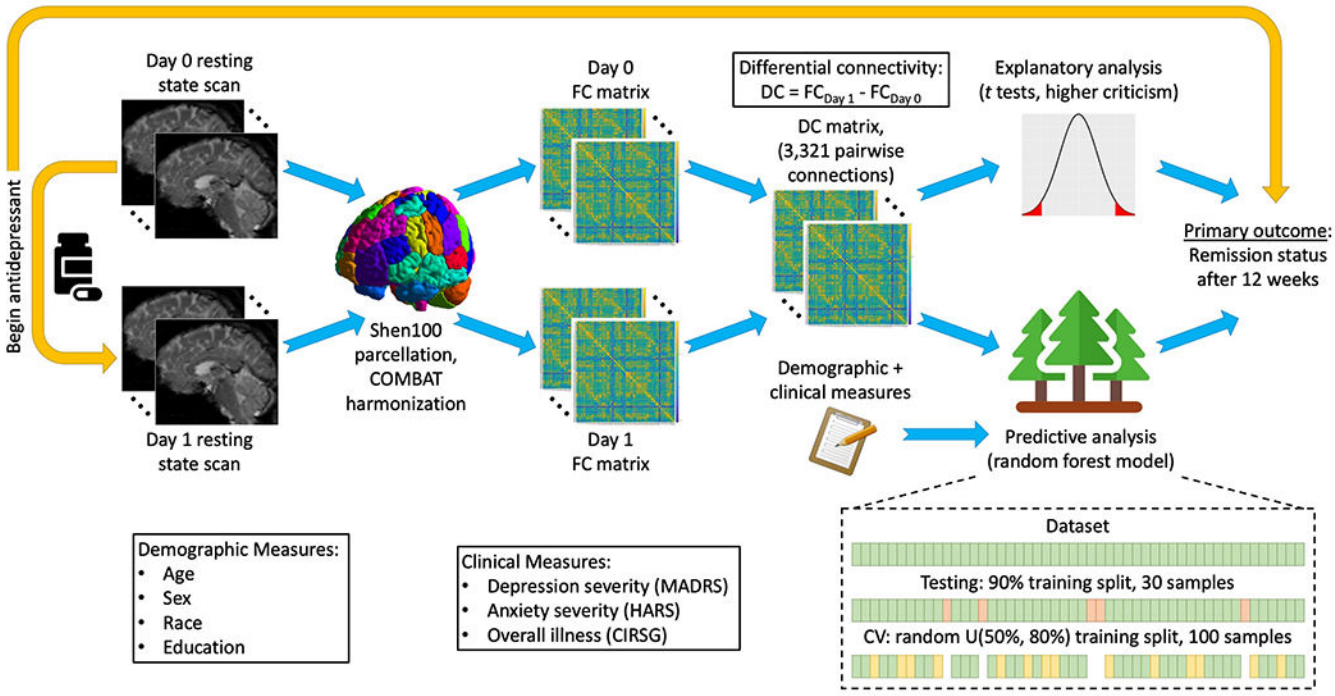

Figure 2. Study design and analysis flow chart.

FC – functional connectivity, DC – differential connectivity, CV – cross-validation.

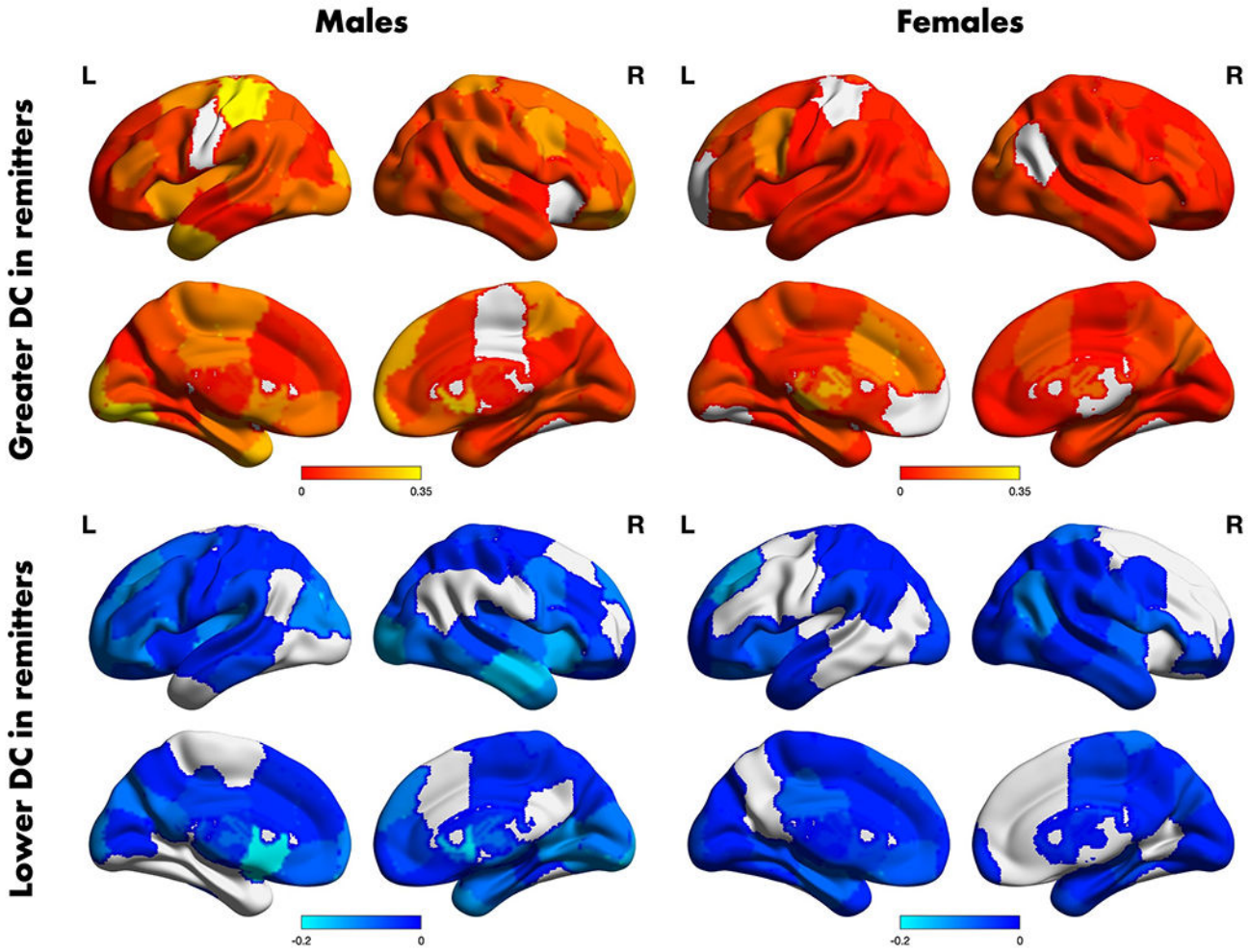

Figure 3. Regional differential connectivity summary differences between remitters and non-remitters according to sex.

The *t*-statistic map of the region-wise average positive (top row) and negative (bottom row) differences in day 1 differential connectivity among remitters and non-remitters according to sex. Only edges with $p < 0.05$ (uncorrected) were included in the average. Figures were visualized using the *BrainNet Viewer* software in Matlab v. 2020b.

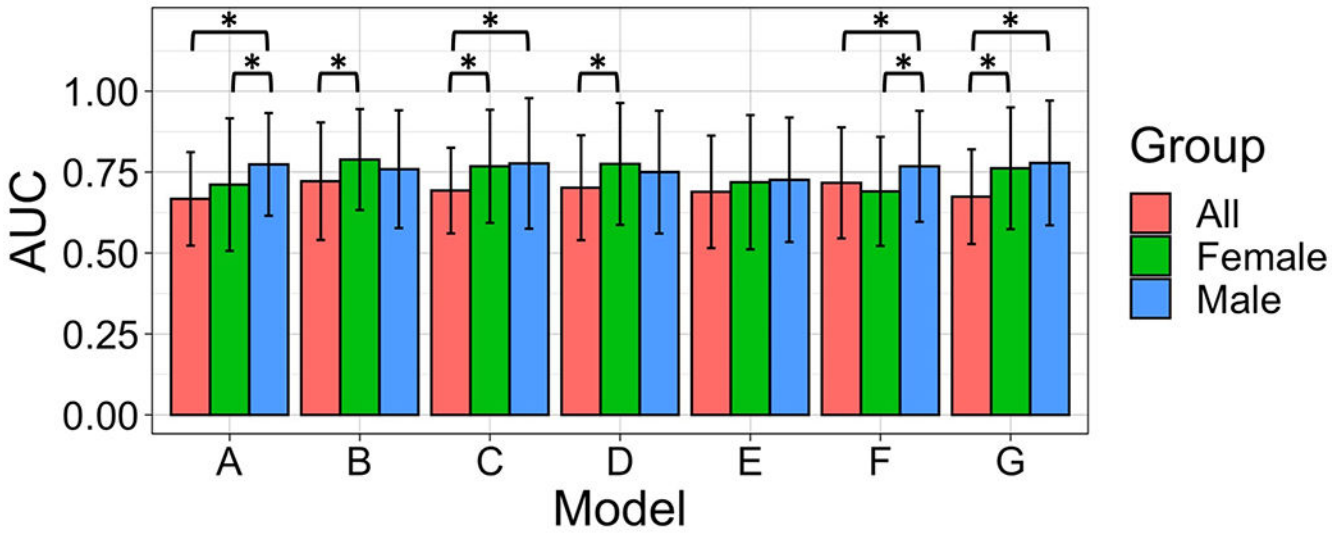

Figure 4. Prediction performance of models to predict remitter status.

The mean and standard deviation of the Accuracy Under the Curve (AUC) of fitted random forest models across all individuals, females-only, and males-only participants in the pooled cohort. Error bars represent the standard deviation of the AUC across 30 repetitions. Asterisks (*) indicate a statistically significant difference in mean predictive AUCs between model*s* from a two-sample t-test at the 0.05 significance level (Bonferroni correction accounting for 3 pairwise comparisons of each model).

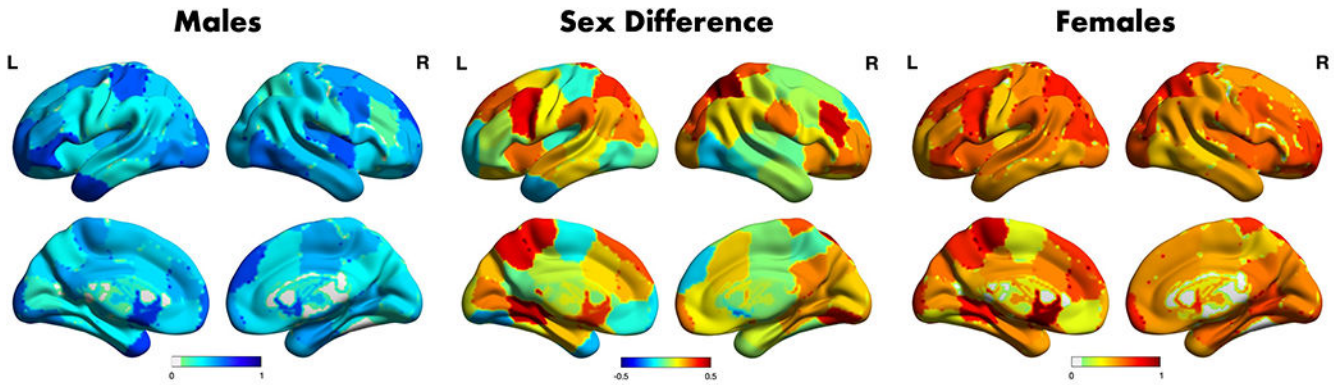

Figure 5. Differential Connectivity Importance for Prediction of Remission.

Edge-wise permutation variable importance values from model F were *z*-scored to allow comparison across models and averaged across each region. These normalized region-wise average permutation variable importance values for the prediction of remission status are shown for the male-only model (left) and female-only model (right). Sex differences (females minus males) of the normalized region-wise average importance values are also shown (center). Figures were visualized using the BrainNet Viewer software in Matlab v. 2020b.

Table 1:

Description of variables incorporated in each of the predictive models for treatment response.

Variables	Model						
	A	B	C	D	E	F	G
Demographic (age, sex, race, education level)	x	x	x	x	x	x	x
Clinical (CIRS-G, scanner)	x	x	x	x	x	x	x
Depression symptomatology (MADRS, HARS)	x			x		x	x
Baseline connectivity (3486 edge variables)		x		x	x		x
Differential connectivity (3486 edge variables)			x		x	x	x

Table 2:

Demographic and clinical summaries of the combined participants in the study broken down by sex. Bolded test statistics signify statistical differences between male and female groups at a 0.05 level of significance.

Characteristic	Males	Females	Test Statistic
Total Participants, n (%)	**31 (38.7)**	**49 (61.3)**	**$\chi^2_1 = 7.23$, $p = 0.007$**
Age, Mean (SD)	66.06 (8.5)	66.27 (5.5)	$t_{58} = -0.12$, $p = 0.905$
Black/African American, n (%)	4 (12.9)	11 (22.4)	$\chi^2_1 = 0.60$, $p = 0.480$
Education Years, Mean (SD)	15.77 (2.7)	15.04(2.5)	$t_{58} = 1.17$, $p = 0.248$
Treatment, n (%)	Escitalopram 9 (29.0) Levomilnacipran 4 (12.9) Venlafaxine 18 (58.1)	Escitalopram 14 (28.6) Levomilnacipran 2 (4.1) Venlafaxine 33 (67.3)	$\chi^2_1 = 0$, $p = 1.000$
Baseline MADRS, Mean (SD)	25.81 (7.0)	23.19 (6.3)	$t_{58} = 1.68$, $p = 0.099$
CIRS-G, Mean (SD)	9.80 (3.6)	9.30 (4.6)	$t_{58} = 0.54$, $p = 0.592$
Remitters, n (%)	12 (38.7)	30 (61.2)	$\chi^2_1 = 3.01$, $p = 0.083$

Table 3.

The five regions with the highest average variable importance predicting remission for males and females.

	Shen Region	Anatomical Region	Variable Importance
Females	L_BA48_1	L Caudate	0.0125
	L_BA7_2	L Paracentral Lobule	0.0106
	L_BA19_2	L Lingual Gyrus	0.0094
	R_BA7_3	R Superior/Inferior Parietal Lobe	0.0092
	L_BA7_1	L Superior Parietal Lobe	0.0091
Males	L_BA48_1	L Caudate	0.0069
	L_BA38_1	L Inferior/Middle Temporal Pole	0.0068
	L_BA47_1	L Inferior Frontal Gyrus	0.0067
	R_BA9_1	R Superior Medial/Dorsolateral Prefrontal Cortex	0.0066
	R_BA48_1	R Caudate	0.0066